Supplement 1

Extrusion Calculation: Prior to 1995, Mount Hope Bay larval sampling was conducted using a 505-µm mesh net. From 1995 onward, to avoid loss of winter flounder larvae due to extrusion, sampling during the dominant winter flounder larval period was done with a 333-µm mesh net. Further, both meshes were used simultaneously in a dual bongo frame, each frame with its own flow meter, to then construct year-specific extrusion factors. The time series average of these extrusion factors was then used to calibrate annual average larval abundances prior to 1995 to account for larvae likely extruded with the coarser mesh and provide a consistent time series for comparison with the Narragansett Bay survey.

Table S1. Dual mesh data summary from the Mount Hope Bay survey. Annual average winter flounder densities for each mesh, and the ratio of the two catches (i.e. extrusion factor). The time series average extrusion factor was used for standardizing the time series and accounting for extruded larvae. The time series mean is presented with the standard deviation.

Year	505-µm (# 100m^3)	333-µm (# 100m^3)	Extrusion Factor (333-µm:505-µm)
1995	173.1	299.2	1.73
1996	24.4	63.6	2.61
1997	45.7	70.5	1.54
1998	13.7	29.9	2.18
1999	29.3	42.3	1.44
2000	17.0	28.1	1.65
2001	33.4	45.9	1.38
2002	33.7	57.4	1.70
2003	13.0	23.8	1.83
2004	25.9	59.1	2.28
2005	14.4	28.5	1.98
2006	25.4	45.9	1.81
2007	32.4	38.6	1.19
2008	18.0	33.5	1.86
2009	13.4	20.9	1.57
2010	8.2	22.3	2.71
2011	7.6	22.9	3.00
2012	11.4	21.2	1.87
2013	22.9	47.0	2.05
2014	10.0	27.2	2.72
2015	13.3	35.4	2.66
2016	26.2	46.9	1.79
2017	17.2	35.3	2.05
Average	27.37 (±33.22)	49.80 (±56.21)	1.98 (±0.48)

Supplement 2

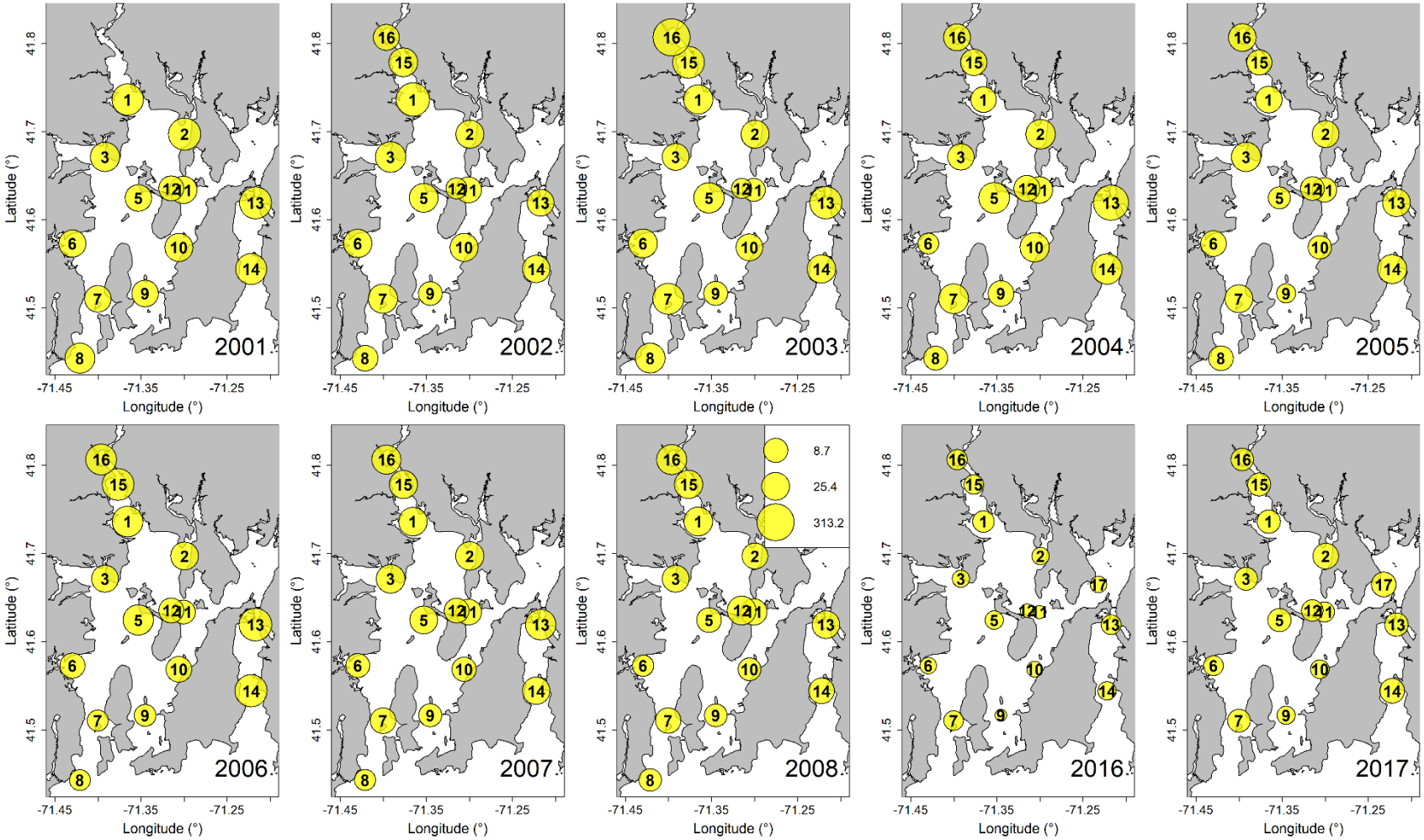

Figure S1. Average winter flounder larval densities by station and year of the Narragansett Bay dataset. Size of points reflect differences in larval densities (no. larvae per 100m^3). All sites by year are included regardless of the sampling consistency through time. Scale of points represent ln(density*100).

Supplement 3

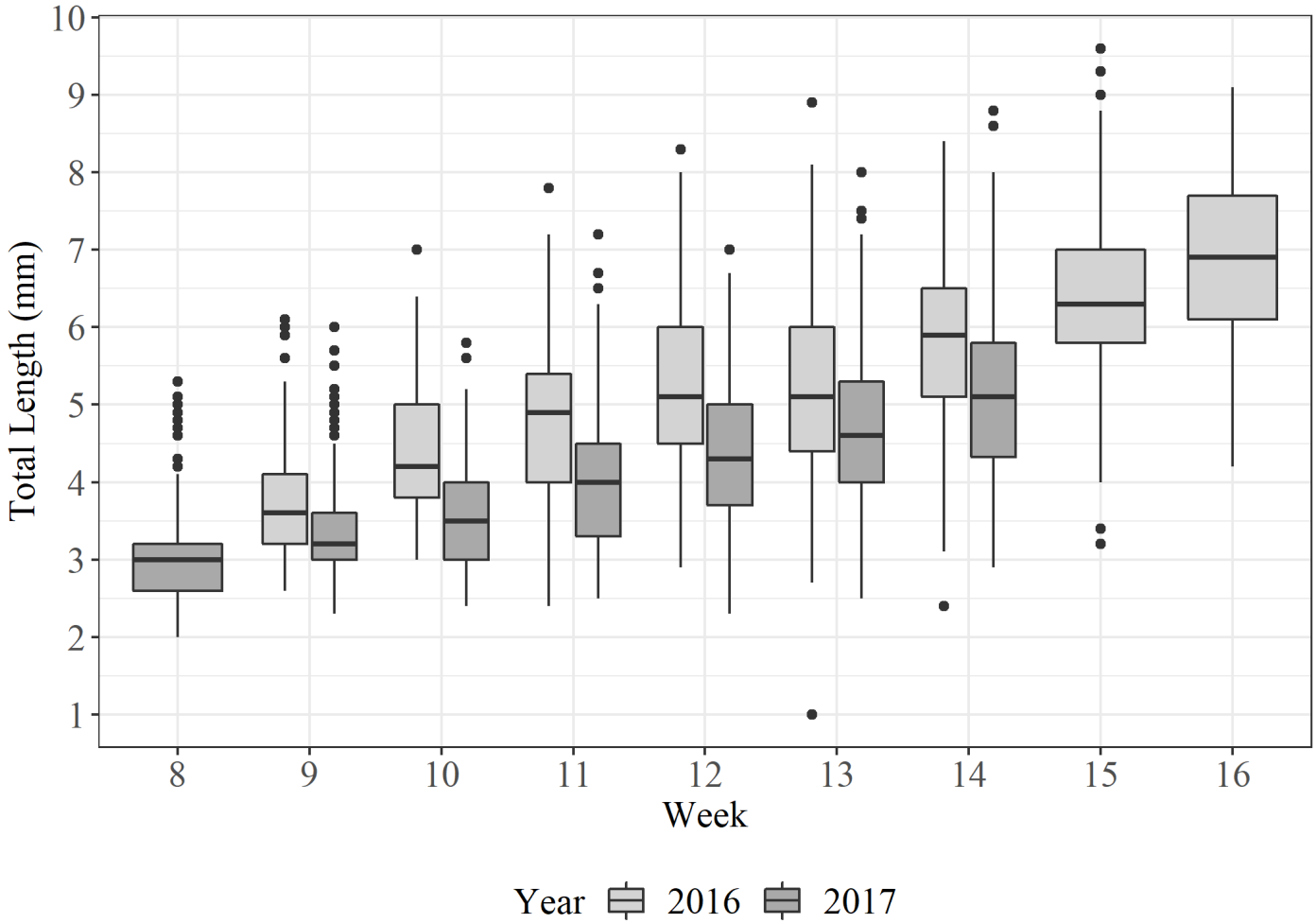

Figure S2. Larval winter flounder size compositions (mm) by week and year for 2016 (mild temperature) and 2017 (colder year). Rectangles and the solid line within them represent the interquartile range (25^{th} , 50^{th}, and 75^{th} percentiles).

Supplement 4.

Generalized additive models (GAMs) were also used to model winter flounder larval densities from the Narragansett Bay survey to understand spatial and environmental drivers on larvae. When using the Narragansett Bay dataset, day of year, station name, and bottom and surface temperatures from the concurrently sampled field data were evaluated; however, bottom and surface temperatures indicated strong collinearity (variance inflation factor > 3), likely reflecting well mixed water columns during the winter period. Thus, only surface temperatures were used in modeling efforts. Similar to the Mount Hope Bay GAM, larval densities were modeled with a Tweedie distribution. The model degrees of freedom in the GCV score were penalized by setting the gamma parameter to 1.4 to reduce model overfitting without degrading prediction error performance (Wood, 2006). Surface temperature and day of year were modeled as continuous variables with thin plate regression splines, and station was modeled as a fixed effect.

The Tweedie GAM for winter flounder larval density in Narragansett Bay also explained 51% of the deviance. Densities were highest after late February through April, and when sea surface temperatures were between approximately 5-11°C (Figure S3). The station effect highlighted similar patterns as the empirical data. The northern stations in the Providence River (1 and 16) had positive effects on the larval densities, while the southerly stations tended to have negative effects on larval density (Figure S3). Sakonnet River sites deviated from this apparent latitudinal effect the greatest. This pattern was further highlighted when regressing the site effects against their station latitude external to the GAM, with a significant positive linear response between the two variables (least squares regression R^2=0.23, p<0.033).

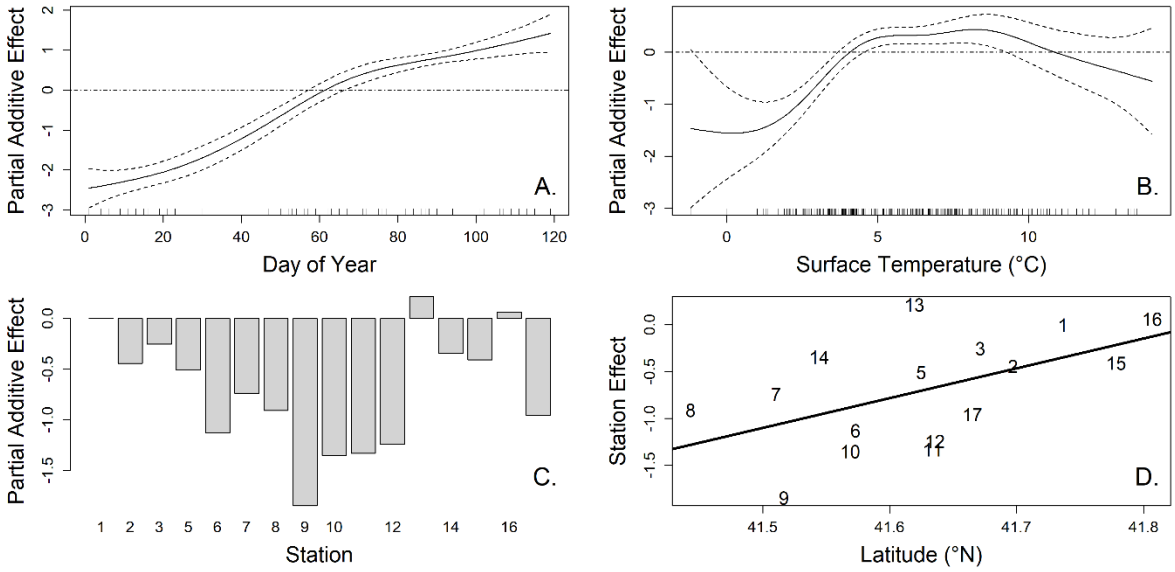

Figure S3. GAM results for predicting winter flounder larval densities from the Narragansett Bay dataset. Fit relations for larval density model with day of the year (A), surface temperature (B), and unique station (C). The correlation between station effects and latitude are also presented (D).

Supplement 5.

Larval length information were available for the 2016 and 2017 Narragansett Bay survey data, and were examined to describe the spawning and larval hatch timing and infer whether larvae were spawned locally, either within sites or more broadly (i.e. Narragansett Bay or external spawning with larvae transport to the Bay). While winter flounder ecology suggests that Narragansett Bay larvae are spawned and retained locally, larval transport modeling indicates larval connectivity may exist between distant areas (DeCelles et al. 2015). Daily ages were estimated for larvae using previously reported larval growth curves (Jearld et al. 1993), with hatching dates calculated by subtracting larval ages from the days of the year the samples were taken.

Winter flounder larval lengths sampled in 2016 and 2017 were between 1.0 and 9.6 mm, with fifty percent of observed larvae between 3.3 and 5.3 mm and a median of 4.2 mm (Figure S5). Using the growth rate from Jearld et al. (1993), the larval size range corresponded to larval ages between 1 and 73 days old. The median age for larvae was 16 days old, with fifty percent of observed larvae between 12 and 21 days old (Figure S4). Hatch day estimates indicated that larvae were spawned between mid-January through early-April. In 2016, the median hatch day was March 9, approximately 2 weeks later than 2017 (Figure S4.)

The smallest larval sizes observed corresponded to typical hatch sizes for larvae of approximately 2.4 mm (Fahay 1983.) These size and age estimates suggest that observed larvae were spawned within Narragansett Bay and close to where they were observed. This conclusion is based on the age estimation, which can vary as a function of temperature-dependent growth (Laurence 1975; Able and Fahay 1998.) Thus, development of time-varying or environmentally explicit growth curves would aid in confirming this postulation.

LITERATURE CITED

DeCelles G, Cowles G, Liu C, Cadrin S (2015) Modeled transport of winter flounder larvae spawned in coastal waters of the Gulf of Maine. Fish Oceanogr. 24(5):430-444.

Fahay, M (1983) Guide to the early stages of marine fishes occuring in the Western North Atlantic Ocean, Cape Hatteras to the Southern Scotian Shelf. J. Northwest Atl. Fish. Sci. 4: 1-423.

Jearld A, Sass SL, Davis MF (1993) Early growth, behavior, and otolith development of the winter flounder Pleuronectes americanus. Fish Bull 91:65–75.

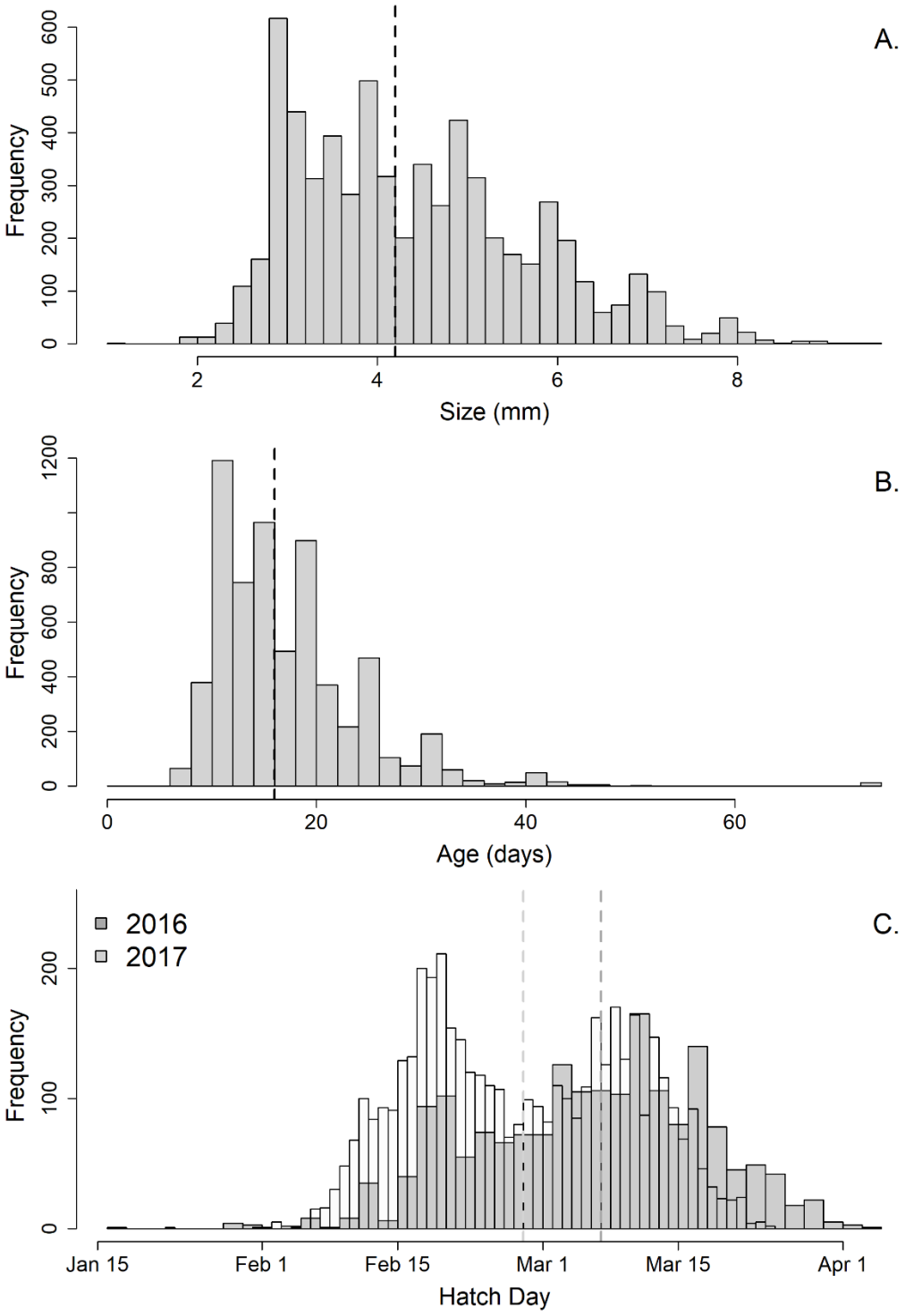

Figure S4. Larval winter flounder size distribution (A) and estimated age composition (B) in 2016 and 2017, and estimated day of hatch for 2016 and 2017 (C). Vertical dashed lines represent the median size (A), age (B), and hatch days (C) of the larval catch. In 2016, temperatures were warmer than 2017.